Received: 14 May 2021 | Accepted: 1 June 2021

DOI: 10.1002/pip.3444

ACCELERATED PUBLICATION

PROGRESS IN PHOTOVOLTAICS WILEY

Solar cell efficiency tables (Version 58)

Martin A. Green[1] | Ewan D. Dunlop[2] | Jochen Hohl-Ebinger[3] | Masahiro Yoshita[4] | Nikos Kopidakis[5] | Xiaojing Hao[1]

[1]School of Photovoltaic and Renewable Energy Engineering, Australian Centre for Advanced Photovoltaics, University of New South Wales, Sydney, New South Wales, Australia

[2]Directorate C – Energy, Transport and Climate, European Commission – Joint Research Centre, Ispra, Italy

[3]Department of Characterisation and Simulation/CalLab Cells, Fraunhofer Institute for Solar Energy Systems, Freiburg, Germany

[4]Renewable Energy Research Center (RENRC), National Institute of Advanced Industrial Science and Technology (AIST), Tsukuba, Ibaraki, Japan

[5]PV Cell and Module Performance, National Renewable Energy Laboratory, Golden, Colorado, USA

Correspondence
Martin A. Green, School of Photovoltaic and Renewable Energy Engineering, Australian Centre for Advanced Photovoltaics, University of New South Wales, Sydney, NSW 2052, Australia.
Email: m.green@unsw.edu.au

Funding information
Japanese New Energy and Industrial Technology Development Organisation (NEDO); U.S. Department of Energy (Office of Science, Office of Basic Energy Sciences and Energy Efficiency and Renewable Energy, Solar Energy Technology Program), Grant/Award Number: DE-AC36-08-GO28308; Australian Government through the Australian Renewable Energy Agency (ARENA)

Abstract

Consolidated tables showing an extensive listing of the highest independently confirmed efficiencies for solar cells and modules are presented. Guidelines for inclusion of results into these tables are outlined, and new entries since January 2021 are reviewed.

KEYWORDS
energy conversion efficiency, photovoltaic efficiency, solar cell efficiency

1 | INTRODUCTION

Since January 1993, *Progress in Photovoltaics* has published six monthly listings of the highest confirmed efficiencies for a range of photovoltaic cell and module technologies.[1,2] By providing guidelines for inclusion of results into these tables, this not only provides an authoritative summary of the current state of the art but also encourages researchers to seek independent confirmation of results and to report results on a standardised basis. In Version 33 of these tables,[2] results were updated to the new internationally accepted reference spectrum (International Electrotechnical Commission IEC 60904-3, Ed. 2, 2008).

The most important criterion for inclusion of results into the tables is that they must have been independently measured by a recognised test centre listed in an earlier issue.[1] A distinction is made between three different eligible definitions of cell area: total area, aperture area and designated illumination area, as defined in an earlier issue[1] (note that, if masking is used, masks must have a simple

TABLE 1 Confirmed single-junction terrestrial cell and submodule efficiencies measured under the global AM1.5 spectrum (1000 W/m^2) at 25°C (IEC 60904-3: 2008 or ASTM G-173-03 global)

Classification	Efficiency (%)	Area (cm^2)	V_{oc} (V)	J_{sc} (mA/cm^2)	Fill factor (%)	Test centre (date)	Description
Silicon							
Si (crystalline cell)	26.7 ± 0.5	79.0 (da)	0.738	42.65[a]	84.9	AIST (3/17)	Kaneka, n-type rear IBC[3]
Si (DS wafer cell)	24.4 ± 0.3	267.5 (t)	0.7132	41.47[b]	82.5	ISFH (8/20)	Jinko Solar, n-type
Si (thin transfer submodule)	21.2 ± 0.4	239.7 (ap)	0.687[c]	38.50[c,d]	80.3	NREL (4/14)	Solexel (35 μm thick)[4]
Si (thin-film minimodule)	10.5 ± 0.3	94.0 (ap)	0.492[c]	29.7[c,e]	72.1	FhG-ISE (8/07)	CSG Solar (<2 μm on glass)[5]
III–V cells							
GaAs (thin-film cell)	29.1 ± 0.6	0.998 (ap)	1.1272	29.78[f]	86.7	FhG-ISE (10/18)	Alta Devices[6]
GaAs (multicrystalline)	18.4 ± 0.5	4.011 (t)	0.994	23.2	79.7	NREL (11/95)	RTI, Ge substrate[7]
InP (crystalline cell)	24.2 ± 0.5[g]	1.008 (ap)	0.939	31.15[a]	82.6	NREL (3/13)	NREL[8]
Thin-film chalcogenide							
CIGS (cell) (Cd-free)	23.35 ± 0.5	1.043 (da)	0.734	39.58[h]	80.4	AIST (11/18)	Solar Frontier[9]
CIGSSe (submodule)	**19.6 ± 0.5**	**670.6 (ap)**	**0.688**	**37.63**[i]	**75.8**	**NREL (2/21)**	**Avancis, 110 cells**[10]
CdTe (cell)	21.0 ± 0.4	1.0623 (ap)	0.8759	30.25[d]	79.4	Newport (8/14)	First Solar, on glass[11]
CZTSSe (cell)	11.3 ± 0.3	1.1761 (da)	0.5333	33.57[f]	63.0	Newport (10/18)	DGIST, Korea[12]
CZTS (cell)	10.0 ± 0.2	1.113 (da)	0.7083	21.77[a]	65.1	NREL (3/17)	UNSW[13]
Amorphous/microcrystalline							
Si (amorphous cell)	10.2 ± 0.3[j,g]	1.001 (da)	0.896	16.36[d]	69.8	AIST (7/14)	AIST[14]
Si (microcrystalline cell)	11.9 ± 0.3[g]	1.044 (da)	0.550	29.72[a]	75.0	AIST (2/17)	AIST[15]
Perovskite							
Perovskite (cell)	**22.6 ± 0.6**[k]	**1.0189 (da)**	**1.178**	**22.73**[i]	**84.4**	**CSIRO (10/20)**	**ANU**[16]
Perovskite (minimodule)	**20.1 ± 0.4**[k]	**63.98 (da)**	**1.155**[c]	**23.09**[c,i]	**75.4**	**JET (3/21)**	**UtmoLight, 12 cells**[17]
Dye sensitised							
Dye (cell)	11.9 ± 0.4[l]	1.005 (da)	0.744	22.47[m]	71.2	AIST (9/12)	Sharp[18]
Dye (minimodule)	10.7 ± 0.4[l]	26.55 (da)	0.754[c]	20.19[c,n]	69.9	AIST (2/15)	Sharp, 7 serial cells[18]
Dye (submodule)	8.8 ± 0.3[l]	398.8 (da)	0.697[c]	18.42[c,o]	68.7	AIST (9/12)	Sharp, 26 serial cells[18]
Organic							
Organic (cell)	15.2 ± 0.2[g,p]	1.015 (da)	0.8467	24.24[b]	74.3	FhG-ISE (10/20)	Fraunhofer ISE
Organic (minimodule)	**13.6 ± 0.3**[p]	**66.62 (da)**	**0.8283**[c]	**23.85**[c,i]	**68.7**	**ESTI (5/21)**	**WAYS/Nanobit/NCU (16 cells)**
Organic (submodule)	11.7 ± 0.2[p]	203.98 (da)	0.8177[c]	20.68[c,q]	69.3	FhG-ISE (10/19)	ZAE Bayern (33 cells)[19]

Abbreviations: (ap), aperture area; (da), designated illumination area; (t), total area; AIST, Japanese National Institute of Advanced Industrial Science and Technology; a-Si, amorphous silicon/hydrogen alloy; CIGS, $CuIn_{1-y}Ga_ySe_2$; CZTS, Cu_2ZnSnS_4; CZTSSe, $Cu_2ZnSnS_{4-y}Se_y$; DS, directionally solidified (including mono cast and multicrystalline); FhG-ISE, Fraunhofer Institut für Solare Energiesysteme; nc-Si, nanocrystalline or microcrystalline silicon.

[a]Spectral response and current–voltage curve reported in Version 50 of these tables.

[b]Spectral response and current–voltage curve reported in Version 57 of these tables.

[c]Reported on a 'per-cell' basis.

[d]Spectral responses and current–voltage curve reported in Version 45 of these tables.

[e]Recalibrated from original measurement.

[f]Spectral response and current–voltage curve reported in the Version 53 of these tables.

[g]Not measured at an external laboratory.

[h]Spectral response and current–voltage curve reported in Version 54 of these tables.

[i]Spectral response and current–voltage curve reported in present version of these tables.

[j]Stabilised by 1000-h exposure to one-sun light at 50°C.

[k]Initial performance. References[20,21] review the stability of similar devices.

[l]Initial efficiency. Reference[22] reviews the stability of similar devices.

[m]Spectral response and current–voltage curve reported in Version 41 of these tables.

[n]Spectral response and current–voltage curve reported in Version 46 of these tables.
[o]Spectral response and current–voltage curve reported in Version 43 of these tables.
[p]Initial performance. References[23–25] review the stability of similar devices.
[q]Spectral response and current–voltage curve reported in Version 55 of these tables.

TABLE 2 'Notable exceptions' for single-junction cells and submodules: 'Top dozen' confirmed results, not class records, measured under the global AM1.5 spectrum (1000 W/m^2) at 25°C (IEC 60904-3: 2008 or ASTM G-173-03 global)

Classification	Efficiency (%)	Area (cm^2)	V_{oc} (V)	J_{sc} (mA/cm^2)	Fill factor (%)	Test centre (date)	Description
Cells (silicon)							
Si (crystalline)	**25.0 ± 0.5**	**4.00 (da)**	**0.706**	**42.7**[a]	**82.8**	**Sandia (3/99)**	**UNSW, p-type PERC**[26]
Si (crystalline)	25.8 ± 0.5[b]	4.008 (da)	0.7241	42.87[c]	83.1	FhG-ISE (7/17)	FhG-ISE, n-type **TOPCon**[27]
Si (crystalline)	26.0 ± 0.5[b]	4.015 (da)	0.7323	42.05[d]	82.3	FhG-ISE (11/19)	FhG-ISE, p-type **TOPCon**
Si (crystalline)	26.1 ± 0.3[b]	3.9857 (da)	0.7266	42.62[e]	84.3	ISFH (2/18)	ISFH, p-type rear IBC[28]
Si (large crystalline)	24.0 ± 0.3	244.59 (t)	0.6940	41.58[f]	83.3	ISFH (7/19)	LONGi, p-type PERC[29]
Si (large crystalline)	**25.2 ± 0.4**	**242.97 (ap)**	**0.7216**	**41.64**[g]	**83.9**	**ISFH (5/21)**	**LONGi, n-type TOPCon**[30]
Si (large crystalline)	**25.3 ± 0.4**	**244.53 (ap)**	**0.7485**	**39.48**[g]	**85.5**	**ISFH (5/21)**	**LONGi, n-type HJT**[31]
Si (large crystalline)	26.6 ± 0.5	179.74 (da)	0.7403	42.5[h]	84.7	FhG-ISE (11/16)	Kaneka, n-type rear IBC[3]
Cells (III–V)							
GaInP	22.0 ± 0.3[b]	0.2502 (ap)	1.4695	16.63[i]	90.2	NREL (1/19)	NREL, rear HJ, strained AlInP[32]
Cells (chalcogenide)							
CdTe (thin film)	22.1 ± 0.5	0.4798 (da)	0.8872	31.69[j]	78.5	Newport (11/15)	First Solar on glass[33]
CZTSSe (thin film)	12.6 ± 0.3	0.4209 (ap)	0.5134	35.21[k]	69.8	Newport (7/13)	IBM solution grown[34]
CZTS (thin film)	11.0 ± 0.2	0.2339 (da)	0.7306	21.74[h]	69.3	NREL (3/17)	UNSW on glass[35]
Cells (other)							
Perovskite (thin film)	25.5 ± 0.8[l,m]	0.0954 (ap)	1.1885	25.74[f]	83.2	Newport (7/20)	UNIST Ulsan[36]
Organic (thin film)	18.2 ± 0.2[n]	0.0322 (da)	0.8965	25.72[f]	78.9	NREL (10/20)	SJTU Shanghai/Beihang U.
Dye sensitised	12.25 ± 0.4[o]	0.0963 (ap)	1.0203	15.17[d]	79.1	Newport (8/19)	EPFL[37]

Abbreviations: (ap), aperture area; (da), designated illumination area; (t), total area; AIST, Japanese National Institute of Advanced Industrial Science and Technology; CIGSSe, CuInGaSSe; CZTS, Cu_2ZnSnS_4; CZTSSe, $Cu_2ZnSnS_{4-y}Se_y$; DS, directionally solidified (including mono cast and multicrystalline); FhG-ISE, Fraunhofer Institut für Solare Energiesysteme; ISFH, Institute for Solar Energy Research, Hamelin; NREL, National Renewable Energy Laboratory.
[a]Spectral response reported in Version 36 of these tables.
[b]Not measured at an external laboratory.
[c]Spectral response and current–voltage curves reported in Version 51 of these tables.
[d]Spectral response and current–voltage curves reported in Version 55 of these tables.
[e]Spectral response and current–voltage curve reported in Version 52 of these tables.
[f]Spectral response and current–voltage curves reported in Version 57 of these tables.
[g]Spectral response and current–voltage curve reported in the present version of these tables.
[h]Spectral response and current–voltage curves reported in Version 50 of these tables.
[i]Spectral response and current–voltage curve reported in Version 54 of these tables.
[j]Spectral response and/or current–voltage curves reported in Version 46 of these tables.
[k]Spectral response and current–voltage curves reported in Version 44 of these tables.
[l]Stability not investigated. References[20,21] document stability of similar devices.
[m]Measured using 10-point IV sweep with constant voltage bias until current change rate < 0.07%/min.
[n]Long-term stability not investigated. References[23–25] document stability of similar devices.
[o]Long-term stability not investigated. Reference[22] documents stability of similar devices.

TABLE 3 Confirmed multiple-junction terrestrial cell and submodule efficiencies measured under the global AM1.5 spectrum (1000 W/m^2) at 25°C (IEC 60904-3: 2008 or ASTM G-173-03 global)

Classificatio	Efficiency (%)	Area (cm^2)	V_{oc} (V)	J_{sc} (mA/cm^2)	Fill factor (%)	Test centre (date)	Description
III–V multijunctions							
5-junction cell (bonded) (2.17/1.68/1.40/1.06/.73 eV)	38.8 ± 1.2	1.021 (ap)	4.767	9.564	85.2	NREL (7/13)	Spectrolab, 2-terminal[38]
InGaP/GaAs/InGaAs	37.9 ± 1.2	1.047 (ap)	3.065	14.27[a]	86.7	AIST (2/13)	Sharp, 2 term.[39]
GaInP/GaAs (monolithic)	32.8 ± 1.4	1.000 (ap)	2.568	14.56[b]	87.7	NREL (9/17)	LG Electronics, 2 term.
Multijunctions with c-Si							
GaInP/GaInAsP/Si (wafer bonded)	**35.9 ± 1.3[c]**	**3.987 (ap)**	**3.248**	**13.11[d]**	**84.3**	**FhG-ISE (4/20)**	**Fraunhofer ISE, 2-term.**
GaInP/GaAs/Si (mech. stack)	35.9 ± 0.5[c]	1.002 (da)	2.52/0.681	13.6/11.0	87.5/78.5	NREL (2/17)	NREL/CSEM/EPFL, 4-term.[40]
GaInP/GaAs/Si (monolithic)	25.9 ± 0.9[c]	3.987 (ap)	2.647	12.21[e]	80.2	FhG-ISE (6/20)	Fraunhofer ISE, 2-term.[41]
GaAsP/Si (monolithic)	23.4 ± 0.3	1.026 (ap)	1.732	17.34[f]	77.7	NREL (5/20)	OSU/UNSW/SolAero, 2-term[42]
GaAs/Si (mech. stack)	32.8 ± 0.5[c]	1.003 (da)	1.09/0.683	28.9/11.1[g]	85.0/79.2	NREL (12/16)	NREL/CSEM/EPFL, 4-term.[43]
Perovskite/Si (2-terminal)	**29.5 ± 0.5[h]**	**1.121 (da)**	**1.884**	**20.26[d]**	**77.3**	**NREL (12/20)**	**Oxford PV**
GaInP/GaInAs/Ge; Si (spectral split minimodule)	34.5 ± 2.0	27.83 (ap)	2.66/0.65	13.1/9.3	85.6/79.0	NREL (4/16)	UNSW/Azur/Trina, 4-term.[44]
Other multijunctions							
Perovskite/CIGS	24.2 ± 0.7[h]	1.045 (da)	1.768	19.24[f]	72.9	FhG-ISE (1/20)	HZB, 2-terminal[45]
Perovskite/perovskite	24.2 ± 0.8[h]	1.041 (da)	1.986	15.93[f]	76.6	JET (12/19)	Nanjing U, 2-term.[46]
a-Si/nc-Si/nc-Si (thin film)	14.0 ± 0.4[i,c]	1.045 (da)	1.922	9.94[j]	73.4	AIST (5/16)	AIST, 2-term.[47]
a-Si/nc-Si (thin-film cell)	12.7 ± 0.4[i,c]	1.000 (da)	1.342	13.45[k]	70.2	AIST (10/14)	AIST, 2-term.[48]
Notable exceptions							
GaInP/GaAs	32.9 ± 0.5[c]	0.250 (ap)	2.500	15.36[l]	85.7	NREL (1/20)	NREL, multiple QW
GaInP/GaAs/GaInAs	37.8 ± 1.4	0.998 (ap)	3.013	14.60[l]	85.8	NREL (1/18)	Microlink (ELO)[49]
6-junction (monolithic) (2.19/1.76/1.45/1.19/.97/.7 eV)	39.2 ± 3.2[c]	0.247 (ap)	5.549	8.457[m]	83.5	NREL (11/18)	NREL, inv. metamorphic[50]
Perovskite/perovskite	**26.4 ± 0.8[h]**	**0.0494 (da)**	**2.048**	**16.54[d]**	**77.9**	**JET (2/21)**	**Nanjing U, 2-term.[46]**
GaInP/AlGaAs/CIGS	**28.1 ± 1.2[c]**	**0.1386 (da)**	**2.952**	**11.72[d]**	**81.1**	**AIST (1/21)**	**AIST/FhG-ISE, 2-term.[51]**

Abbreviations: (ap), aperture area; (da), designated illumination area; (t), total area; AIST, Japanese National Institute of Advanced Industrial Science and Technology; a-Si, amorphous silicon/hydrogen alloy; FhG-ISE, Fraunhofer Institut für Solare Energiesysteme; nc-Si, nanocrystalline or microcrystalline silicon.

[a]Spectral response and current–voltage curve reported in Version 42 of these tables.
[b]Spectral response and current–voltage curve reported in the Version 51 of these tables.
[c]Not measured at an external laboratory.
[d]Spectral response and current–voltage curve reported in the present version of these tables.
[e]Spectral response and current–voltage curve reported in Version 57 of these tables.
[f]Spectral response and current–voltage curve reported in Version 56 of these tables.
[g]Spectral response and current–voltage curve reported in Version 52 of these tables.
[h]Initial efficiency. References[20,21] review the stability of similar perovskite-based devices.
[i]Stabilised by 1000-h exposure to one-sun light at 50°C.
[j]Spectral response and current–voltage curve reported in Version 49 of these tables.

[k]Spectral responses and current–voltage curve reported in Version 45 of these tables.
[l]Spectral response and current–voltage curve reported in Version 53 of these tables.
[m]Spectral response and current–voltage curve reported in Version 54 of these tables.

TABLE 4 Confirmed non-concentrating terrestrial module efficiencies measured under the global AM1.5 spectrum (1000 W/m^2) at a cell temperature of 25°C (IEC 60904-3: 2008 or ASTM G-173-03 global)

Classification	Effic. (%)	Area (cm^2)	V_{oc} (V)	I_{sc} (A)	FF (%)	Test centre (date)	Description
Si (crystalline)	24.4 ± 0.5	13,177 (da)	79.5	5.04[a]	80.1	AIST (9/16)	Kaneka (108 cells)[3]
Si (multicrystalline)	20.4 ± 0.3	14,818 (ap)	39.90	9.833[b]	77.2	FhG-ISE (10/19)	Hanwha Q Cells (60 cells)[52]
GaAs (thin film)	25.1 ± 0.8	866.45 (ap)	11.08	2.303[c]	85.3	FhG-ISE (11/17)	Alta Devices[53]
CIGS (Cd free)	19.2 ± 0.5	841 (ap)	48.0	0.456[c]	73.7	AIST (1/17)	Solar Frontier (70 cells)[54]
CdTe (thin film)	19.0 ± 0.9	23,573 (da)	227.8	2.560[b]	76.6	FhG-ISE (9/19)	First Solar[55]
a-Si/nc-Si (tandem)	12.3 ± 0.3[d]	14,322 (t)	280.1	0.902[e]	69.9	ESTI (9/14)	TEL Solar, Trubbach Labs[56]
Perovskite	17.9 ± 0.5[f]	804 (da)	58.7	0.323[g]	76.1	AIST (1/20)	Panasonic (55 cells)[57]
Organic	8.7 ± 0.3[h]	802 (da)	17.47	0.569[i]	70.4	AIST (5/14)	Toshiba[58]
Multijunction							
InGaP/GaAs/InGaAs	31.2 ± 1.2	968 (da)	23.95	1.506	83.6	AIST (2/16)	Sharp (32 cells)[59]
Notable exception							
CIGS (large)	18.6 ± 0.6	10,858 (ap)	58.00	4.545[b]	76.8	FhG-ISE (10/19)	Miasole[60]

Abbreviations: (ap), aperture area; (da), designated illumination area; (t), total area; a-Si, amorphous silicon/hydrogen alloy; a-SiGe, amorphous silicon/germanium/hydrogen alloy; CIGSS, CuInGaSSe; Effic., efficiency; FF, fill factor; nc-Si, nanocrystalline or microcrystalline silicon.
[a]Spectral response and current voltage curve reported in Version 49 of these tables.
[b]Spectral response and current–voltage curve reported in Version 55 of these tables.
[c]Spectral response and current–voltage curve reported in Version 50 or 51 of these tables.
[d]Stabilised at the manufacturer to the 2% level following IEC procedure of repeated measurements.
[e]Spectral response and/or current–voltage curve reported in Version 46 of these tables.
[f]Initial performance. References[15,18] review the stability of similar devices.
[g]Spectral response and current–voltage curve reported in Version 57 of these tables.
[h]Initial performance. References[20,21] review the stability of similar devices.
[i]Spectral response and current–voltage curve reported in Version 45 of these tables.

aperture geometry, such as square, rectangular or circular). 'Active area' efficiencies are not included. There are also certain minimum values of the area sought for the different device types (above 0.05 cm^2 for a concentrator cell, 1 cm^2 for a one-sun cell, 800 cm^2 for a module and 200 cm^2 for a 'submodule').

Results are reported for cells and modules made from different semiconductors and for subcategories within each semiconductor grouping (e.g., crystalline, polycrystalline or directionally solidified and thin film). From Version 36 onwards, spectral response information is included (when possible) in the form of a plot of the external quantum efficiency (EQE) versus wavelength, either as absolute values or normalised to the peak measured value. Current–voltage (IV) curves have also been included where possible from Version 38 onwards. A graphical summary of progress over the 28 years during which the tables have been published is included in an earlier issue.[1]

Highest confirmed 'one-sun' cell and module results are reported in Tables 1–4. Any changes in the tables from those previously published[1] are set in bold type. In most cases, a literature reference is provided that describes either the result reported or a similar result (readers identifying improved references are welcome to submit to the lead author). Table 1 summarises the best reported measurements for 'one-sun' (non-concentrator) single-junction cells and submodules.

Table 2 contains what might be described as 'notable exceptions' for 'one-sun' single-junction cells and submodules in the above category. While not conforming to the requirements to be recognised as a class record, the devices in Table 2 have notable characteristics that will be of interest to sections of the photovoltaic community, with entries based on their significance and timeliness. To encourage discrimination, the table is limited to nominally 12 entries with the present authors having voted for their preferences for inclusion. Readers who have suggestions of notable exceptions for inclusion into this or subsequent tables are welcome to contact any of the authors with full details. Suggestions conforming to the guidelines will be included on the voting list for a future issue.

Table 3 was first introduced in Version 49 of these tables and summarises the growing number of cell and submodule results involving high efficiency, one-sun multiple-junction devices (previously reported in Table 1). Table 4 shows the best results for one-sun modules, both single and multiple junctions, whereas Table 5 shows the best results for concentrator cells and concentrator modules. A small number of 'notable exceptions' are also included in Tables 3–5.

TABLE 5 Terrestrial concentrator cell and module efficiencies measured under the ASTM G-173-03 direct beam AM1.5 spectrum at a cell temperature of 25°C, except where noted (also see footnote re relationship to thermodynamic efficiencies)

Classification	Effic. (%)	Area (cm^2)	Intensity[a] (suns)	Test centre (date)	Description
Single cells					
GaAs	30.5 ± 1.0[b]	0.10043 (da)	258	NREL (10/18)	NREL, 1-junction (1J)
Si	27.6 ± 1.2[c]	1.00 (da)	92	FhG-ISE (11/04)	Amonix back-contact[61]
CIGS (thin film)	23.3 ± 1.2[d,e]	0.09902 (ap)	15	NREL (3/14)	NREL[62]
Multijunction cells					
AlGaInP/AlGaAs/GaAs/GaInAs(3) (2.15/1.72/1.41/1.17/0.96/0.70 eV)	47.1 ± 2.6[d,f]	0.099 (da)	143	NREL (3/19)	NREL, 6J inv. metamorphic[48]
GaInP/GaAs; GaInAsP/GaInAs	46.0 ± 2.2[g]	0.0520 (da)	508	AIST (10/14)	Soitec/CEA/FhG-ISE 4J bonded[63]
GaInP/GaAs/GaInAs/GaInAs	45.7 ± 2.3[d,h]	0.09709 (da)	234	NREL (9/14)	NREL, 4J monolithic[64]
InGaP/GaAs/InGaAs	44.4 ± 2.6[i]	0.1652 (da)	302	FhG-ISE (4/13)	Sharp, 3J inverted metamorphic[65]
GaInAsP/GaInAs	35.5 ± 1.2[d,j]	0.10031 (da)	38	NREL (10/17)	NREL 2-junction (2J)[66]
Minimodule					
GaInP/GaAs; GaInAsP/GaInAs	43.4 ± 2.4[d,k]	18.2 (ap)	340[l]	FhG-ISE (7/15)	Fraunhofer ISE 4J (lens/cell)[67]
Submodule					
GaInP/GaInAs/Ge; Si	40.6 ± 2.0[k]	287 (ap)	365	NREL (4/16)	UNSW 4J split spectrum[68]
Modules					
Si	20.5 ± 0.8[d]	1875 (ap)	79	Sandia (4/89)[l]	Sandia/UNSW/ENTECH (12 cells)[69]
Three-junction (3J)	35.9 ± 1.8[m]	1092 (ap)	N/A	NREL (8/13)	Amonix[70]
Four-junction (4J)	38.9 ± 2.5[n]	812.3 (ap)	333	FhG-ISE (4/15)	Soitec[71]
Hybrid module[o]					
4-Junction (4J)/bifacial c-Si	34.2 ± 1.9[d,o]	1088 (ap)	CPV/PV	FhG-ISE (9/19)	FhG-ISE (48/8 cells; 4T)[72]
Notable exceptions					
Si (large area)	21.7 ± 0.7	20.0 (da)	11	Sandia (9/90)[l]	UNSW laser grooved[73]
Luminescent minimodule[o]	7.1 ± 0.2[o]	25 (ap)	2.5[p]	ESTI (9/08)	ECN Petten, GaAs cells[74]
4J minimodule	41.4 ± 2.6[d]	121.8 (ap)	230	FhG-ISE (9/18)	FhG-ISE, 10 cells[67]

Note: Following the normal convention, efficiencies calculated under this direct beam spectrum neglect the diffuse sunlight component that would accompany this direct spectrum. These direct beam efficiencies need to be multiplied by a factor estimated as 0.8746 to convert to thermodynamic efficiencies.[75]

Abbreviations: (ap), aperture area; (da), designated illumination area; CIGS, $CuInGaSe_2$; Effic., efficiency; FhG-ISE, Fraunhofer Institut für Solare Energiesysteme; NREL, National Renewable Energy Laboratory.

[a]One sun corresponds to direct irradiance of 1000 W/m^2.

[b]Spectral response and current–voltage curve reported in Version 53 of these tables.

[c]Measured under a low aerosol optical depth spectrum similar to ASTM G-173-03 direct.[76]

[d]Not measured at an external laboratory.

[e]Spectral response and current–voltage curve reported in Version 44 of these tables.

[f]Spectral response and current–voltage curve reported in Version 54 of these tables.

[g]Spectral response and current–voltage curve reported in Version 45 of these tables.

[h]Spectral response and current–voltage curve reported in Version 46 of these tables.

[i]Spectral response and current–voltage curve reported in Version 42 of these tables.

[j]Spectral response and current–voltage curve reported in Version 51 of these tables.

[k]Determined at IEC 62670-1 CSTC reference conditions.

[l]Recalibrated from original measurement.

[m]Referenced to 1000 W/m^2 direct irradiance and 25°C cell temperature using the prevailing solar spectrum and an in-house procedure for temperature translation.

[n]Measured under IEC 62670-1 reference conditions following the current IEC power rating draft 62670-3.

[o]Thermodynamic efficiency. The hybrid module was measured under the ASTM G-173-03 or IEC 60904-3: 2008 global AM1.5 spectrum at a cell temperature of 25°C. Four-terminal module with external dual-axis tracking. Power rating of CPV follows IEC 62670-3 standard, front power rating of flat plate PV based on IEC 60904-3, -5, -7, -10 and 60891 with modified current translation approach and rear power rating of flat plate PV based on IEC TS 60904-1-2 and 60891.

[p]Geometric concentration.

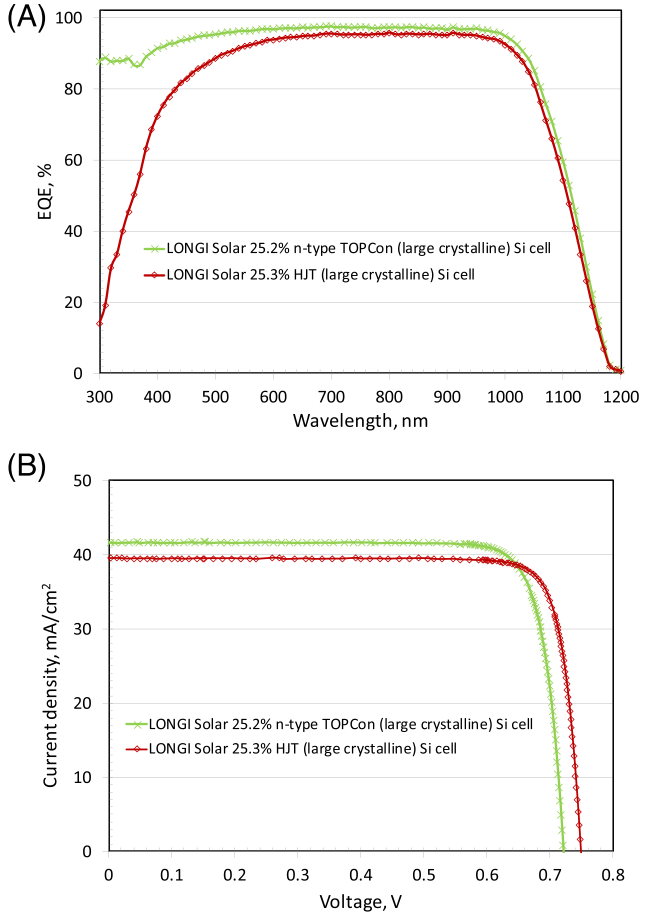

FIGURE 1 (A) External quantum efficiency (EQE) for the new Si cell results reported in this issue. (B) Corresponding current density–voltage (JV) curves [Colour figure can be viewed at wileyonlinelibrary.com]

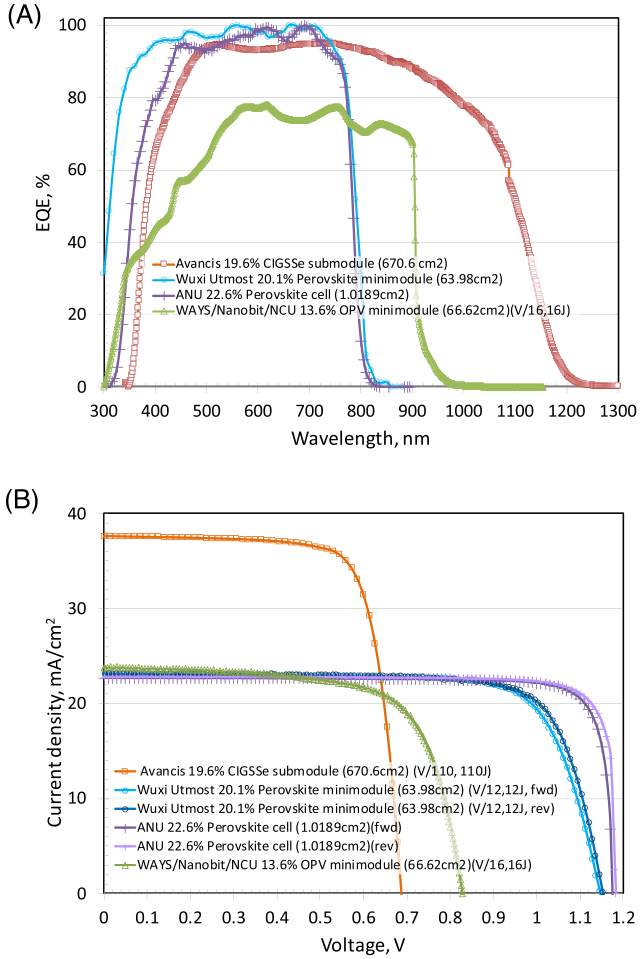

FIGURE 2 (A) External quantum efficiency (EQE) for the new perovskite cell and minimodule plus new CIGS submodule results reported in this issue (some results are normalised). (B) Corresponding current density–voltage (JV) curves [Colour figure can be viewed at wileyonlinelibrary.com]

2 | NEW RESULTS

Ten new results are reported in the present version of these tables. The first new result in Table 1 ('one-sun cells and submodules') is 19.6% efficiency for a large (671 cm^2) $CuIn_{1-x}Ga_xS_2$ (CIGS) submodule fabricated by Avancis, with the result confirmed by the US National Renewable Energy Laboratory (NREL). The submodule, only slightly too small for classification as a module (>800 cm^2), is based on a CIGS absorber, a sodium-based post-treatment of the absorber and a cadmium-free sputtered zinc oxysulphide window layer.[10]

The second new result in Table 1 is a new efficiency record for a perovskite solar cell of a reasonable size. An efficiency of 22.6% is reported for a 1-cm^2 cell fabricated by the Australian National University (ANU) and measured at the Commonwealth Scientific and Industrial Research Organisation (CSIRO). The cell uses a nanostructured TiO_2 electron transport layer that modifies the spatial distribution of the passivation layer to form nanoscale localised charge transport pathways through an otherwise passivated interface, therefore providing both effective passivation and good charge extraction.[16] The third new result is a landmark 20.1% efficiency for a 64-cm^2 perovskite minimodule fabricated by Wuxi Utmost Light Technology Co. Ltd (UtmoLight)[17] and measured at the Japan Electrical Safety and Environment Technology Laboratories (JET). Along with other emerging technologies, perovskite cells and modules may not demonstrate the same level of stability as more established cell technologies, with references to this aspect given in the footnotes to Table 1. The final new result in Table 1 is 13.6% efficiency for a 67-cm^2 organic photovoltaic (OPV) minimodule fabricated by Ways, Nanobit and the National Central University (NCU) of Taiwan and measured at the European Solar Test Installation (ESTI).

The silicon results in Table 2 (one-sun 'notable exceptions') have been reorganised to incorporate representation from the four cell technologies presently battling for commercial supremacy (PERC, TOPCon, HJT and IBC). PERC is the 'passivated emitter and rear cell', originally developed at UNSW Sydney,[26] presently accounting for over 90% of commercial production. TOPCon stands for 'tunnel oxide passivated contact', generally referring to contact at the cell rear (not top!). In the version of commercial interest, it involves cell contacting by tunnelling through a thin oxide from a doped polysilicon layer, an

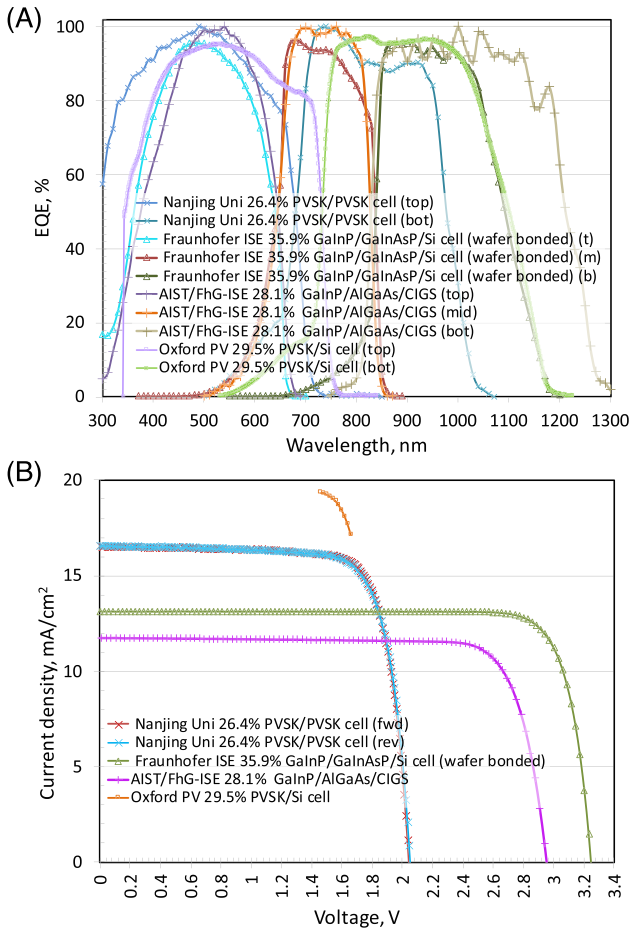

FIGURE 3 (A) External quantum efficiency (EQE) for the new multijunction cell results reported in this issue (some results are normalised). (B) Corresponding current density–voltage (JV) curves (only portion of the Oxford PV curve shown due to measurement approach) [Colour figure can be viewed at wileyonlinelibrary.com]

approach first suggested and demonstrated by UNSW Sydney[77] but more recently revitalised and developed to commercial readiness by the Fraunhofer Institute for Solar Energy Systems (FhG-ISE).[78] HJT ('heterojunction') cells have evolved from the HIT ('heterojunction with intrinsic thin-layer') cells originally developed by Sharp,[79] involving contacting each side of a high-quality, uniformly doped silicon wafer by a thin, wider bandgap hydrogenated amorphous silicon layer of opposite polarity.[80] IBC stands for 'interdigitated back contact', an approach first suggested by Lammert and Schwartz[81] and subsequently developed by Stanford University[82] and Sunpower.[83]

The first of two new results in Table 2 is a total area efficiency of 25.2% for a large area (243-cm^2) n-type silicon TOPCon cell fabricated by LONGi Solar[30] and measured by the Institute für Solarenergieforschung (ISFH). The second new result in this table is an increase in efficiency to 25.3% for a large area (245-cm^2) n-type HJT silicon cell again fabricated by LONGi Solar[31] and also measured by ISFH. Due to the reporting changes noted above, an earlier result for a 25.0% efficient p-type 4-cm^2 silicon cell, fabricated by UNSW Sydney[26] and measured at Sandia National Laboratories, is also reinstated as the most efficient PERC cell yet fabricated.

Four new results are reported in Table 3 relating to one-sun, multijunction devices. Improvements are reported for a 4-cm^2 two-terminal, triple-junction $Ga_{0.51}In_{0.49}P/Ga_{0.93}In_{0.07}As_{0.87}P_{0.13}$//Si solar cell of 35.9% efficiency fabricated and certified at FhG-ISE, where the silicon cell is wafer bonded to the overlying III–V cell combination[40] (the '//' symbol represents the wafer bond location). The second new result is for a perovskite/Si tandem device. An efficiency of 29.5% has been confirmed for a 1-cm^2 device fabricated by Oxford PV[83] and measured by NREL.

The final two results are included as 'notable exceptions'. One is for an all-perovskite tandem device where an efficiency of 26.4% was measured for a small area 0.049-cm^2 perovskite/perovskite two-junction, two-terminal device fabricated by Nanjing University[46] and measured by JET. The final result for a 0.14-cm^2 two-terminal, triple-junction GaInP/AlGaAs/CIS solar cell of 28.1% efficiency[51] fabricated jointly by the Japanese National Institute of Advanced Industrial Science and Technology (AIST) and FhG-ISE and certified by AIST. Cell area in both cases is too small for classification as an outright record, with solar cell efficiency targets in governmental research programmes generally specified in terms of a cell area of 1 cm^2 or larger.[84–86]

The EQE spectra for the new silicon cells reported in the present issue of these tables are shown in Figure 1A, with Figure 1B showing the current density–voltage (JV) curves for the same devices. Figure 2A,B shows the corresponding EQE and JV curves for the new organic and perovskite cell and minimodule results, whereas Figure 3A,B shows these for the new multijunction cell results.

DISCLAIMER

Although the information provided in the tables is provided in good faith, the authors, editors and publishers cannot accept direct responsibility for any errors or omissions.

ACKNOWLEDGEMENTS

The Australian Centre for Advanced Photovoltaics commenced operation in February 2013 with support from the Australian Government through the Australian Renewable Energy Agency (ARENA). The Australian Government does not accept responsibility for the views, information or advice expressed herein. The work at NREL was supported by the U.S. Department of Energy under Contract No. DE-AC36-08-GO28308 with the National Renewable Energy Laboratory. The work at AIST was supported in part by the Japanese New Energy and Industrial Technology Development Organisation (NEDO) under the Ministry of Economy, Trade and Industry (METI).

ORCID

Martin A. Green https://orcid.org/0000-0002-8860-396X

REFERENCES

1. Green MA, Dunlop ED, Hohl-Ebinger J, Yoshita M, Kopidakis N, Hao XJ. Solar cell efficiency tables (Version 57). *Prog Photovolt: Res Appl*. 2021;29(1):3-15.

2. Green MA, Emery K, Hishikawa Y, Warta W. Solar cell efficiency tables (Version 33). *Prog Photovolt: Res Appl*. 2009;17(1):85-94.
3. Yoshikawa K, Kawasaki H, Yoshida W, et al. Silicon heterojunction solar cell with interdigitated back contacts for a photoconversion efficiency over 26%. *Nat Energy*. 2017;2(5):17032.
4. Moslehi MM, Kapur P, Kramer J, et al. World-record 20.6% efficiency 156 mm × 156 mm full-square solar cells using low-cost kerfless ultrathin epitaxial silicon & porous silicon lift-off technology for industry-leading high-performance smart PV modules. In: *PV Asia Pacific Conference (APVIA/PVAP)*, 24 October; 2012.
5. Keevers MJ, Young TL, Schubert U, Green MA. 10% efficient CSG minimodules. In: *22nd European Photovoltaic Solar Energy Conference*. Milan, September; 2007.
6. Kayes BM, Nie H, Twist R, et al. 27.6% conversion efficiency, a new record for single-junction solar cells under 1 sun illumination. In: *Proceedings of the 37th IEEE Photovoltaic Specialists Conference*; 2011.
7. Venkatasubramanian R, O'Quinn BC, Hills JS, et al. 18.2% (AM1.5) efficient GaAs solar cell on optical-grade polycrystalline Ge substrate. In: *Conference Record, 25th IEEE Photovoltaic Specialists Conference*. Washington, May; 1997:31-36.
8. Wanlass M. Systems and methods for advanced ultra-high-performance InP solar cells. In: *US Patent 9,590,131 B2*, 7 March; 2017.
9. Nakamura M, Yamaguchi K, Kimoto Y, Yasaki Y, Kato T, Sugimoto H. Cd-free Cu (In,Ga)(Se,S)2 thin-film solar cell with a new world record efficacy of 23.35%, *46th IEEE PVSC*, Chicago, IL, June 19, 2019 (see also http://www.solar-frontier.com/eng/news/2019/0117_press.html
10. Diermann R. Avancis claims 19.64% efficiency for CIGS module, *PV Magazine International*, March 4, 2021. (https://www.pv-magazine.com/2021/03/04/avancis-claims-19-64-efficiency-for-cigs-module/
11. First Solar Press Release, First Solar builds the highest efficiency thin film PV cell on record, 5 August 2014.
12. https://en.dgist.ac.kr/site/dgist_eng/menu/984.do (accessed 28 October 2018).
13. Yan C, Huang J, Sun K, et al. $Cu_2ZnSn\ S_4$ solar cells with over 10% power conversion efficiency enabled by heterojunction heat treatment. *Nat Energy*. 2018;3(9):764-772.
14. Matsui T, Bidiville A, Sai H, et al. High-efficiency amorphous silicon solar cells: impact of deposition rate on metastability. *Appl Phys Lett*. 2015;106(5):053901. https://doi.org/10.1063/1.4907001
15. Sai H, Matsui T, Kumagai H, Matsubara K. Thin-film microcrystalline silicon solar cells: 11.9% efficiency and beyond. *Appl Phys Express*. 2018;11(2):022301.
16. Peng J, Walter D, Ren Y, et al. Nanoscale localized contacts for high fill factors in polymer-passivated perovskite solar cells. *Science*. 2021;371(6527):390-395.
17. Chinese Perovskite Tech Firm Wuxi Utmost Light Claims 20.5% 'World Record' Efficiency For Perovskite Solar Mini-Module, Certified By Japan's JET; Plans To Build Large-Area Perovskite Solar Module Production Lines, http://taiyangnews.info/technology/20-5-world-record-efficiency-for-perovskite-solar-module/
18. Komiya R, Fukui A, Murofushi N, Koide N, Yamanaka R, Katayama H. Improvement of the conversion efficiency of a monolithic type dye-sensitized solar cell module. In: *Technical Digest, 21st International Photovoltaic Science and Engineering Conference*. Fukuoka, November; 2011 2C-5O-08.
19. New world record efficiency for organic solar modules, https://www.encn.de/fileadmin/user_upload/PR_opv-record__.pdf (accessed 11 November 2019).
20. Han Y, Meyer S, Dkhissi Y, et al. Degradation observations of encapsulated planar $CH_3NH_3PbI_3$ perovskite solar cells at high temperatures and humidity. *J Mater Chem A*. 2015;3(15):8139-8147.
21. Yang Y, You J. Make perovskite solar cells stable. *Nature*. 2017;544(7649):155-156.
22. Krašovec UO, Bokalič M, Topič M. Ageing of DSSC studied by electroluminescence and transmission imaging. *Solar Energy Mater Solar Cells*. 2013;117:67-72.
23. Tanenbaum DM, Hermenau M, Voroshazi E, et al. The ISOS-3 inter-laboratory collaboration focused on the stability of a variety of organic photovoltaic devices. *RSC Adv*. 2012;2(3):882-893.
24. Krebs FC (Ed). *Stability and Degradation of Organic and Polymer Solar Cells*. Chichester: Wiley; 2012.
25. Jorgensen M, Norrman K, Gevorgyan SA, Tromholt T, Andreasen B, Krebs FC. Stability of polymer solar cells. *Adv Mater*. 2012;24:580-612.
26. Green MA. The Passivated Emitter and Rear Cell (PERC): from conception to mass production. *Solar Energy Mater Solar Cells*. 2015;143:190-197.
27. Richter A, Benick J, Feldmann F, Fell A, Hermle M, Glunz SW. n-Type Si solar cells with passivating electron contact: identifying sources for efficiency limitations by wafer thickness and resistivity variation. *Solar Energy Mater Solar Cells*. 2017;173:96-105.
28. Haase F, Klamt C, Schäfer S, et al. Laser contact openings for local poly-Si-metal contacts enabling 26.1%-efficient POLO-IBC solar cells. *Solar Energy Mater Solar Cells*. 2018;186:184-193.
29. Wang Q. Status of crystalline silicon PERC solar cells. In: *NIST/UL Workshop on Photovoltaic Materials Durability*. Gaithersburg, MD USA, Dec 12–13; 2019.
30. LONGi sets record of 25.09% for N-Type TOPCon cell efficiency. https://en.longi-solar.com/home/events/press_detail/id/331.html
31. LONGi breaks three more world records for solar cell efficiency. *Press Release*, 2 June 2021. https://en.longi-solar.com/home/events/press_detail/id/335.html
32. NREL, private communication, 22 May 2019.
33. First Solar Press Release. First Solar Achieves yet another cell conversion efficiency world record, 24 February 2016.
34. Wang W, Winkler MT, Gunawan O, et al. Device characteristics of CZTSSe thin-film solar cells with 12.6% efficiency. *Adv Energy Mater*. 2014;4(7):1301465. https://doi.org/10.1002/aenm.201301465
35. Sun K, Yan C, Liu F, et al. Beyond 9% efficient kesterite Cu_2ZnSnS_4 solar cell: fabricated by using $Zn_{1-x}Cd_xS$ buffer layer. *Adv Energy Mater*. 2016;6(12):1600046. https://doi.org/10.1002/aenm.201600046
36. Jeong M, Choi IW, Go EM, et al. Stable perovskite solar cells with efficiency exceeding 24.8% and 0.3-V voltage loss. *Science*. 2020;369(6511):1615-1620. https://doi.org/10.1126/science.abb7167
37. https://www.epfl.ch/labs/lspm/; https://www.epfl.ch/labs/lpi/ (accessed 28 October 2019).
38. Chiu PT, Law DL, Woo RL, et al. 35.8% space and 38.8% terrestrial 5J direct bonded cells. *Proc. 40th IEEE Photovoltaic Specialist Conference, Denver*. 2014:11-13.
39. Sasaki K, Agui T, Nakaido K, Takahashi N, Onitsuka R, Takamoto T. Proceedings, 9th International Conference on Concentrating Photovoltaics Systems, Miyazaki, Japan 2013.
40. Müller R, Schygulla P, Lackner D, et al. Silicon-based monolithic triple-junction solar cells with conversion efficiency >34%. *37th European Photovoltaic Solar Energy Conference and Exhibition*, pp: 574–578 DOI: https://doi.org/10.4229/EUPVSEC20202020-3AO.7.2
41. Feifel M, Lackner D, Ohlmann J, Benick J, Hermle M, Dimroth F. Direct growth of a GaInP/GaAs/Si triple-junction solar cell with 22.3% AM1.5G efficiency. *Sol RRL*. 3(1–7):1900313. https://doi.org/10.1002/solr.201900313
42. Grassman TJ, Chmielewski DJ, Carnevale SD, Carlin JA, Ringel SA. GaAs0.75 P0.25/Si dual-junction solar cells grown by MBE and MOCVD. *IEEE J Photovolt*. 2016;6(1):326-331.

43. Essig S, Allebé C, Remo T, et al. Raising the one-sun conversion efficiency of III–V/Si solar cells to 32.8% for two junctions and 35.9% for three junctions. *Nat Energy*. 2017;2(9):17144. https://doi.org/10.1038/nenergy.2017.144
44. Green MA, Keevers MJ, Concha Ramon B, et al. Improvements in sunlight to electricity conversion efficiency: above 40% for direct sunlight and over 30% for global. Paper 1AP.1.2. In: *European Photovoltaic Solar Energy Conference 2015*. Hamburg, September; 2015.
45. HZB hits 23.26% efficiency with CIGS-perovskite tandem cell, https://www.pv-magazine.com/2019/09/11/hzb-hits-23-26-efficiency-with-cigs-perovskite-tandem-cell/ (accessed 28 October 2019).
46. Lin R, Xiao K, Qin ZY, et al. Monolithic all-perovskite tandem solar cells with 24.8% efficiency exploiting comproportionation to suppress Sn (ii) oxidation in precursor ink. *Nat Energy*. 2019;4(10):864-873.
47. Sai H, Matsui T, Koida T, Matsubara K. Stabilized 14.0%-efficient triple-junction thin-film silicon solar cell. *Appl Phys Lett*. 2016;109(18):183506. https://doi.org/10.1063/1.49669986
48. Matsui T, Maejima K, Bidiville A, et al. High-efficiency thin-film silicon solar cells realized by integrating stable a-Si:H absorbers into improved device design. *Jpn J Appl Phys*. 2015;54:08KB10. https://doi.org/10.7567/JJAP.54.08KB10
49. MicroLink AFWERX Phase I Projects, http://mldevices.com/index.php/news/ (accessed 28 October 2018).
50. Geisz JF, Steiner MA, Jain N, et al. Building a six-junction inverted metamorphic concentrator solar cell. *IEEE J Photovolt*. 2018;8(2):626-632.
51. Makita K, Kamikawa Y, Mizuno H, et al. III-V//$Cu_xIn_{1-y}Ga_ySe_2$ multijunction solar cells with 27.2% efficiency fabricated using modified smart stack technology with Pd nanoparticle array and adhesive material. *Prog Photovolt: Res Appl*. in press. https://doi-org.wwwproxy1.library.unsw.edu.au/10.1002/pip.3398
52. https://www.hanwha-qcells.com (accessed 28 October 2019)
53. Mattos LS, Scully SR, Syfu M, Olson E, Yang L, Ling C, Kayes BM, He G. New module efficiency record: 23.5% under 1-sun illumination using thin-film single-junction GaAs solar cells. Proceedings of the 38th IEEE Photovoltaic Specialists Conference, 2012.
54. Sugimoto H. High efficiency and large volume production of CIS-based modules. 40th IEEE Photovoltaic Specialists Conference, Denver, June 2014.
55. http://www.firstsolar.com/en-AU/-/media/First-Solar/Technical-Documents/Series-6-Datasheets/Series-6-Datasheet.ashx (accessed 28 October 2019).
56. Cashmore JS, Apolloni M, Braga A, et al. Improved conversion efficiencies of thin-film silicon tandem (MICROMORPH ™) photovoltaic modules. *Solar Energy Mater Solar Cells*. 2016;144:84-95. https://doi.org/10.1016/j.solmat.2015.08.022
57. Higuchi H, Negami T. Largest highly efficient $203 \times 203\ mm^2$ $CH_3NH_3PbI_3$ perovskite solar modules. *Jpn J Appl Phys*. 2018;57:08RE11.
58. Hosoya M, Oooka H, Nakao H, Gotanda T, Mori S, Shida N, Hayase R, Nakano Y, Saito M. Organic thin film photovoltaic modules. Proceedings of the 93rd Annual Meeting of the Chemical Society of Japan 2013; 21–37.
59. Takamoto, T. Application of InGaP/GaAs/InGaAs triple junction solar cells to space use and concentrator photovoltaic. 40th IEEE Photovoltaic Specialists Conference, Denver, June 2014.
60. Bheemreddy V, Liu BJJ, Wills A, Murcia CP. Life prediction model development for flexible photovoltaic modules using accelerated damp heat testing. IEEE 7th World Conf. on Photovoltaic Energy Conversion (WCPEC) 2018: 1249–1251.
61. Slade A, Garboushian V. 27.6% efficient silicon concentrator cell for mass production. In: *Technical Digest, 15th International Photovoltaic Science and Engineering Conference*. Shanghai, October; 2005:701.
62. Ward JS, Ramanathan K, Hasoon FS, et al. A 21.5% efficient Cu(In,Ga)Se2 thin-film concentrator solar cell. *Prog Photovolt: Res Appl*. 2002;10(1):41-46.
63. Dimroth F, Tibbits TND, Niemeyer M, et al. Four-junction wafer-bonded concentrator solar cells. *IEEE J Photovolt* January. 2016;6(1):343-349. https://doi.org/10.1109/JPHOTOV.2015.2501729
64. NREL. *Press Release NR-4514*, 16 December 2014.
65. Press Release, Sharp Corporation, 31 May 2012 (accessed at http://sharp-world.com/corporate/news/120531.html on 5 June 2013).
66. Jain N, Schulte KL, Geisz JF, et al. High-efficiency inverted metamorphic 1.7/1.1 eV GaInAsP/GaInAs dual-junction solar cells. *Appl Phys Lett*. 2018;112:053905.
67. Steiner M, Siefer G, Schmidt T, Wiesenfarth M, Dimroth F, Bett AW. 43% sunlight to electricity conversion efficiency using CPV. *IEEE J Photovolt* July. 2016;6(4):1020-1024. https://doi.org/10.1109/JPHOTOV.2016.2551460
68. Green MA, Keevers MJ, Thomas I, Lasich JB, Emery K, King RR. 40% efficient sunlight to electricity conversion. *Prog Photovolt: Res Appl*. 2015;23(6):685-691.
69. Chiang CJ and Richards EH. A 20% efficient photovoltaic concentrator module. Conf. Record, 21st IEEE Photovoltaic Specialists Conference, Kissimimee, May 1990: 861–863.
70. http://amonix.com/pressreleases/amonix-achieves-world-record-359-module-efficiency-rating-nrel-4 (accessed 23 October 2013).
71. van Riesen S, Neubauer M, Boos A, Rico MM, Gourdel C, Wanka S, Krause R, Guernard P, Gombert A. New module design with 4-junction solar cells for high efficiencies. Proceedings of the 11th Conference on Concentrator Photovoltaic Systems, 2015.
72. Martínez JF, Steiner M, Wiesenfarth M, Siefer G, Glunz SW, Dimroth F. Power rating procedure of hybrid CPV/PV bifacial modules. *Prog Photovolt Res Appl*. 2021;29(6):614-629.
73. Zhang F, Wenham SR, Green MA. Large area, concentrator buried contact solar cells. *IEEE Trans Electron Dev*. 1995;42(1):144-149.
74. Slooff LH, Bende EE, Burgers AR, et al. A luminescent solar concentrator with 7.1% power conversion efficiency. *Phys Stat Sol (RRL)*. 2008;2(6):257-259.
75. Müllejans H, Winter S, Green MA, Dunlop ED. What is the correct efficiency for terrestrial concentrator PV devices? In: *38th European Photovoltaic Solar Energy Conference*, Sept; 2021 (accepted for presentation).
76. Gueymard CA, Myers D, Emery K. Proposed reference irradiance spectra for solar energy systems testing. *Solar Energy*. 2002;73(6):443-467.
77. Green MA, Blakers AW. Advantages of metal-insulator-semiconductor structures for silicon solar cells. *Solar Cells*. 1983;8(1):3-16.
78. Feldmann F, Bivour M, Reichel C, Hermle M, Glunz SW. Passivated rear contacts for high-efficiency n-type Si solar cells providing high interface passivation quality and excellent transport characteristics. *Solar Energy Mater Solar Cells*. 2014;120:270-274.
79. Mishima T, Taguchi M, Sakata H, Maruyama E. Development status of high-efficiency HIT solar cells. *Solar Energy Mater Solar Cells*. 2011;95(1):18-21.
80. Allen TG, Bullock J, Yang X, Javey A, De Wolf S. Passivating contacts for crystalline silicon solar cells. *Nat Energy*. 2019;4(11):914-928.
81. Lammert MD, Schwartz RJ. The interdigitated back contact solar cell: a silicon solar cell for use in concentrated sunlight. *IEEE Trans Electron Devices*. 1977;24(4):337-342.
82. Sinton RA, Swanson RM. Simplified backside-contact solar cells. *IEEE Trans Electron Dev*. 1990;37(2):348-352.
83. Cousins PJ, Smith DD, Luan H-C, Manning J, Dennis TD, Waldhauer A, Wilson KE, Harley G, Mulligan WP. Generation 3: improved performance at lower cost. 35th IEEE Photovoltaic Specialists Conference, Honolulu, 20–25 June 2010.

84. Program milestones and decision points for single junction thin films. Annual Progress Report 1984, Photovoltaics, Solar Energy Research Institute, Report DOE/CE-0128, June 1985, 7.
85. Sakata I, Tanaka Y, Koizawa K. Japan's new national R&D program for photovoltaics. Photovoltaic Energy Conversion, Conference Record of the 2006 IEEE 4th World Conference, Vol 1, May 2008, 1–4.
86. Jäger-Waldau, A (Ed.). *PVNET: European Roadmap for PV R&D, EUR 21087 EN*, 2004.

How to cite this article: Green MA, Dunlop ED, Hohl-Ebinger J, Yoshita M, Kopidakis N, Hao X. Solar cell efficiency tables (Version 58). *Prog Photovolt Res Appl*. 2021;29: 657–667. https://doi.org/10.1002/pip.3444